



**HAL**  
open science

## Smooth muscle $\alpha v$ integrins regulate vascular fibrosis via CD109 downregulation of TGF- $\beta$ signalling

Zhenlin Li, Ekaterina Belozertseva, Ara Parlakian, Rümeyza Bascetin, Huguette Louis, Yuki Kawamura, Jocelyne Blanc, Jacqueline Gao-Li, Florence Pinet, Adam Lacy-Hulbert, et al.

### ► To cite this version:

Zhenlin Li, Ekaterina Belozertseva, Ara Parlakian, Rümeyza Bascetin, Huguette Louis, et al.. Smooth muscle  $\alpha v$  integrins regulate vascular fibrosis via CD109 downregulation of TGF- $\beta$  signalling. *European Heart Journal Open*, 2023, 3 (2), pp.oead010. 10.1093/ehjopen/oead010 . inserm-04026458

**HAL Id: inserm-04026458**

**<https://inserm.hal.science/inserm-04026458>**

Submitted on 13 Mar 2023

**HAL** is a multi-disciplinary open access archive for the deposit and dissemination of scientific research documents, whether they are published or not. The documents may come from teaching and research institutions in France or abroad, or from public or private research centers.

L'archive ouverte pluridisciplinaire **HAL**, est destinée au dépôt et à la diffusion de documents scientifiques de niveau recherche, publiés ou non, émanant des établissements d'enseignement et de recherche français ou étrangers, des laboratoires publics ou privés.

# Smooth muscle $\alpha_v$ integrins regulate vascular fibrosis via CD109 downregulation of TGF- $\beta$ signalling

Zhenlin Li<sup>1</sup>, Ekaterina Belozertseva<sup>2</sup>, Ara Parlakian<sup>1</sup>, Rümeyza Bascetin<sup>2</sup>, Huguette Louis<sup>2</sup>, Yuki Kawamura<sup>3</sup>, Jocelyne Blanc<sup>1</sup>, Jacqueline Gao-Li<sup>1</sup>, Florence Pinet<sup>4</sup>, Adam Lacy-Hulbert<sup>5</sup>, Pascal Challande<sup>6</sup>, Jay D. Humphrey<sup>3</sup>, Veronique Regnault<sup>2,†</sup>, and Patrick Lacolley <sup>2,†\*</sup>

<sup>1</sup>Biological Adaptation and Ageing, Sorbonne Université, CNRS, INSERM, IBPS, 7 quai Saint Bernard, 75005 Paris, France; <sup>2</sup>Université de Lorraine, INSERM, DCAC, F-54000, Nancy, France; <sup>3</sup>Department of Biomedical Engineering and Vascular Biology and Therapeutics Program, Yale University, New Haven, CT, USA; <sup>4</sup>U1167—RID-AGE—Facteurs de risque et déterminants moléculaires des maladies liées au vieillissement, Univ. Lille, CHU Lille, INSERM, Institut Pasteur de Lille, F-59000, Lille, France; <sup>5</sup>Department of Immunology, University of Washington, Seattle, WA, 98109; and <sup>6</sup>Sorbonne Université, CNRS, Institut Jean Le Rond d'Alembert, 4 place Jussieu, 75005, Paris, France

Received 28 April 2022; revised 16 January 2023; accepted 14 February 2023; online publish-ahead-of-print 16 February 2023

Handling Editor: Daniel FJ Ketelhuth

## Aims

$\alpha_v$  integrins are implicated in fibrosis in a number of organs through their ability to activate TGF- $\beta$ . However their role in vascular fibrosis and collagen accumulation is only partially understood. Here we have used  $\alpha_v$  conditional knockout mice and cell lines to determine how  $\alpha_v$  contributes to vascular smooth muscle cell (VSMC) function in vascular fibrosis and the role of TGF- $\beta$  in that process.

## Methods and results

Angiotensin II (Ang II) treatment causes upregulation of  $\alpha_v$  and  $\beta_3$  expression in the vessel wall, associated with increased collagen deposition. We found that deletion of  $\alpha_v$  integrin subunit from VSMCs ( $\alpha_v^{\text{SMKO}}$ ) protected mice against angiotensin II-induced collagen production and assembly. Transcriptomic analysis of the vessel wall in  $\alpha_v^{\text{SMKO}}$  mice and controls identified a significant reduction in expression of fibrosis and related genes in  $\alpha_v^{\text{SMKO}}$  mice. In contrast,  $\alpha_v^{\text{SMKO}}$  mice showed prolonged expression of CD109, which is known to affect TGF- $\beta$  signalling. Using cultured mouse and human VSMCs, we showed that overexpression of CD109 phenocopied knockdown of  $\alpha_v$  integrin, attenuating collagen expression, TGF- $\beta$  activation, and Smad2/3 signalling in response to angiotensin II or TGF- $\beta$  stimulation. CD109 and TGF- $\beta$  receptor were internalized in early endosomes.

## Conclusion

We identify a role for VSMC  $\alpha_v$  integrin in vascular fibrosis and show that  $\alpha_v$  acts in concert with CD109 to regulate TGF- $\beta$  signalling.

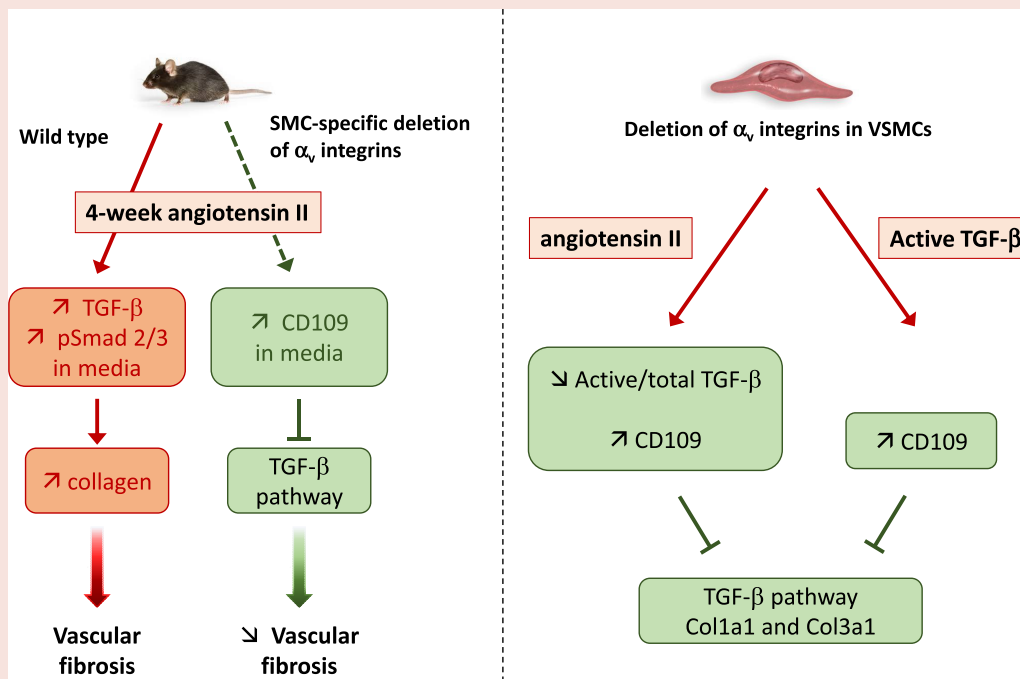
\* Corresponding author. Tel: +33 (0)3 72 74 62 43, Fax: +33 (0)3 72 74 62 52, Email: [patrick.lacolley@inserm.fr](mailto:patrick.lacolley@inserm.fr)

† The first two authors and last two authors participated equally to this work.

© The Author(s) 2023. Published by Oxford University Press on behalf of the European Society of Cardiology.

This is an Open Access article distributed under the terms of the Creative Commons Attribution-NonCommercial License (<https://creativecommons.org/licenses/by-nc/4.0/>), which permits non-commercial re-use, distribution, and reproduction in any medium, provided the original work is properly cited. For commercial re-use, please contact [journals.permissions@oup.com](mailto:journals.permissions@oup.com)

## Graphical Abstract



## Keywords

Alpha v integrin; Vascular smooth muscle cell; Collagen; CD109

## Translational perspective

The role of  $\alpha_v$ -containing integrins in promoting matrix deposition/assembly and synthesis/activation of TGF- $\beta$  in vascular smooth muscle cells (VSMCs) is complex and only partially understood. Here we show that loss of  $\alpha_v$  integrins reduces vascular fibrosis in mice in response to angiotensin II. In angiotensin II-treated cultured VSMCs, loss of  $\alpha_v$  leads to downregulation in matrix and overexpression of membrane-anchored CD109, which in turn reduce TGF- $\beta$  signalling. These data argue that  $\alpha_v$  integrins are components of a core molecular pathway that contributes to TGF- $\beta$  activation and/or regulation of CD109 expression. Interfering with this pathway could limit pathological vascular fibrosis.

## Introduction

Fibrosis, which is hallmarked by excessive accumulation of collagen and other extracellular matrix proteins, is a physiological process involved in tissue repair that can become pathologic.<sup>1</sup> Progressive vascular fibrosis leads to arterial stiffening which is a major independent risk factor for chronic cardiovascular diseases such as hypertension, atherosclerosis, and heart failure.<sup>2,3</sup> Age-related vascular fibrosis and low-grade inflammation are widely accepted as important causes of cardiovascular and overall morbidity and mortality. Although vascular fibrosis is a multicellular process, pheno-modulation of vascular smooth muscle cells (VSMCs) from quiescent to activated fibroblast-like collagen-producing cells is increasingly recognized as a major contributor to vascular fibrosis and stiffening.<sup>3</sup> Cell-extracellular matrix interactions and VSMC phenotypic modulation are fine-tuned by binding of ECM protein to different members of the integrin family which serve as hubs for signal transduction. Among integrins,  $\alpha_v$  integrins (in particular  $\alpha_v\beta_3$ ) has been implicated in VSMC dedifferentiation proliferation, migration, and apoptosis.

Members of the  $\alpha_v$  integrin family are well-established contributors to the activation of transforming growth factor beta (TGF- $\beta$ ).<sup>4</sup> TGF- $\beta$ -activating  $\alpha_v$  integrins have been demonstrated to play a fundamental role on myofibroblasts in regulating lung, liver, kidney, cardiac, and skeletal muscle fibrosis *in vivo*.<sup>5-8</sup> The precise role of  $\alpha_v$  integrin-mediated TGF- $\beta$  activation in vascular fibrosis has not been explored, and in particular whether  $\alpha_v$  integrins are acting through activation of latent TGF- $\beta$  or a different mechanism, such as TGF- $\beta$ /Smad signalling pathway. CD109, a cell-surface glycosylphosphatidylinositol-anchored protein, has been shown to promote TGF- $\beta$ R1 degradation via a ligand-dependent mechanism.<sup>9</sup> CD109 binds to TGF- $\beta$  with high affinity and, thereby enhances the formation of a heteromeric complex with TGF- $\beta$  receptors, directs their compartmentalization and internalization into caveolae, and increases the association of activated TGF- $\beta$  receptors with Smad7/Smad ubiquitination regulatory factor 2 (Smurf2) leading to proteasomal degradation of TGF- $\beta$  receptors.

We hypothesized that CD109 acts negatively on TGF- $\beta$  signalling and fibrotic responses following  $\alpha_v$  integrin-mediated TGF- $\beta$  activation

in VSMCs. We have previously reported that angiotensin II (Ang II) induced a marked upregulation of  $\alpha_v$  subunit gene.<sup>10</sup> Administration of Ang II is a well-established model of vascular fibrosis by stimulating profibrotic and proinflammatory gene expression.<sup>11</sup> We thus evaluated the effect of genetic deletion of the  $\alpha_v$  integrin subunit from VSMCs on Ang II-induced vascular fibrosis using SM22-CreER<sup>T2</sup>(ki)/*Itgav*<sup>fllox/fllox</sup> double-transgenic mice. Therefore, this study combines stimulation of TGF- $\beta$  and knockout of  $\alpha_v$  integrins.

## Methods

### Animals

SM22-CreER<sup>T2</sup>(ki) transgenic mice have been described previously.<sup>12</sup> *Itgav*<sup>fllox/fllox</sup> mice were obtained from A. Lacy-Hulbert<sup>13</sup> and maintained on a C57BL/6 background. *Itgav*<sup>fllox/fllox</sup> mice were crossed with SM22-CreER<sup>T2</sup>(ki) mice to generate SM22-CreER<sup>T2</sup>(ki)/*Itgav*<sup>fllox/fllox</sup> double-transgenic mice. All mice (male and female) were genotyped by PCR as described previously.<sup>12,13</sup> At 8–10 months of age, *Itgav*<sup>fllox/fllox</sup>/SM22-CreER<sup>T2</sup>(ki)/+ mice were injected intraperitoneally with 1 mg of tamoxifen in 100  $\mu$ L of peanut oil for 3 days to generate  $\alpha_v$ <sup>SMKO</sup> mice. *Itgav*<sup>fllox/fllox</sup> littermates injected for 3 days with tamoxifen were used as controls. All experiments were performed 4–6 weeks after tamoxifen injection. Mice were housed in a temperature- and humidity-controlled facility with a 12 h light/day cycle and given free access to standard rodent chow and water. All animal work was conducted in accordance with French regulations and experimental guidelines of the European Community, and the protocols were approved by the local Animal Ethics Committee of the University of Lorraine, France.

### Fibrosis model

The effects of  $\alpha_v$  knockout on gene expression were examined at 6 weeks after tamoxifen injection followed or not by a 4-week treatment with Ang II. Anaesthesia was induced by isoflurane inhalation at 3.5% in 1 L/min oxygen, and then maintained at 1.5% in 1 L/min oxygen during the intervention. Angiotensin II was administered at 1.5 mg/kg/day for 28 days via subcutaneous Alzet osmotic minipumps (Charles River, L'Arbresle, France). Prior to pump implantation, mice were conditioned to tail-cuff blood pressure measurement using a computerized mouse tail-cuff sphygmomanometer (Hatteras Instruments, Inc., NC, USA). Systolic arterial pressure (SAP) and heart rate (HR) were measured on the day of surgery and on day 28 prior to euthanasia. Mice were euthanized via exsanguination under isoflurane anaesthesia (1.5% in 1 L/min oxygen). Carotid arteries were used for morphological and histological analyses and thoracic aorta for all other parameters. It is generally accepted including our previous studies that changes in gene and/or protein expression are similar in these two main conductance arteries.<sup>14,15</sup>

### Histological analysis, immunohistochemistry and immunofluorescence

Histological studies were performed on carotid arteries fixed with 10% buffered formalin under pressure (100 mmHg) *in vivo* for 2 h. Fixed specimens were embedded in paraffin following regular procedures. Five micrometre sections were stained with Sirius Red and Picrosirius Red (PSR) for collagen. PSR sections were imaged under cross-polarized light (darkfield) to observe collagen birefringence. Images were acquired on an Olympus BX/51 microscope using an Olympus DP70 digital camera (cellSens Dimension) under a  $\times 40$  magnification objective. The area fraction of collagen was based on total fibrillar collagen. A custom MATLAB script was used to extract layer-specific (media or

adventitia) wall percentages as well as the proportions of thick (red) and thin (orange–yellow–green) birefringent collagen fibres.<sup>16,17</sup>

For integrin  $\alpha_v$  subunit immunostaining, rabbit polyclonal antibodies against integrin  $\alpha_v$  subunit, biotinylated goat anti-rabbit immunoglobulins, HRP-conjugated streptavidin, and 3,3'-diaminobenzidine (DAB) substrate (see [Supplementary material online, Tables S7 and S8](#)) were used. Composition of the arterial wall and the media cross-sectional area (MCSA) were determined using a Nikon NIS-Elements Basic Research microscope imaging software as described previously.<sup>18</sup>

Immunofluorescence staining on 8  $\mu$ m cryo-sections fixed with 4% paraformaldehyde or cooled acetone for 5 min was performed with specific antibodies as described previously.<sup>14</sup> Briefly, sections were incubated with primary antibodies at 4°C overnight after permeabilization with 0.2% Triton X100 for 10 min and blocking with 5% bovine serum albumin (BSA) for 1 h. After washing in PBS-Tween 20, sections were incubated with fluorescent-conjugated secondary antibodies. A complete list of antibodies is provided in [Supplementary material online, Table S8](#). Image acquisition was on a Leica TCS SP5 confocal microscope (Leica, Wetzlar, Germany) with the same depth of field and with identical settings for laser, gain, and offset intensity.

### Second harmonic generation

The second harmonic generation (SHG) signal was acquired using a femtosecond oscillator (Mira 900F, Coherent), pumped with a solid laser (Verdi 8 W, Coherent) that delivered synchronized pulses (120 fs, 2.5 nJ at 76 MHz) at a wavelength  $\lambda = 800$  nm to a scanning microscope (SP5-CFS, Leica Microsystems, Mannheim, Germany). In the SHG operation mode, the signal was filtered to detect collagen at half the excitation wavelength ( $\lambda/2 = 400$  nm) in the backward direction with a hybrid detector using a large dynamic range combined with low dark noise. The laser beam was focused onto the samples through a dry objective (Leica HC PL FLUOTAR  $\times 10/0.30$ , macroscopic zoom  $\times 16$ ) with the pinhole fully opened to obtain images in matrices  $512 \times 512$  pixels (1 pixel = 1.807  $\mu$ m) at 400 Hz. Native images acquired with Leica LAS-AF software were converted in 32 bit RGB images. The quantitative analyses of collagen fibre directionality and region of interest (ROI) in carotid media were manually selected for each image using ImageJ® software. Second harmonic generation signal was quantified in the grey level by the following equation: grey = (0.299 $\times$ red) + (0.587 $\times$ green) + (0.114 $\times$ blue). Finally, measured signals were normalized accordingly to the number of pixels contained in each ROI for obtaining the mean grey level per pixel.<sup>19</sup>

### Cell culture

Aortic VSMCs were isolated from the descending thoracic aorta of *Itgav*<sup>fllox/fllox</sup> mice. Vascular smooth muscle cells were grown in low-glucose (1 g/L) DMEM/F12 supplemented with 10% foetal bovine serum. Vascular smooth muscle cells were seeded at a density of  $4 \times 10^5$  cells/well into six-well plates and allowed to grow for 24 h to reach about 80% confluence. For  $\alpha_v$  knockdown, VSMCs were transfected with 0.5  $\mu$ L/well of Cre-expressing adenovirus ( $10^{10}$  PFU/mL). For CD109 overexpression, VSMCs were transfected with 0.5  $\mu$ L/well of an adenovirus expressing mouse CD109 ( $10^{10}$  PFU/mL) and containing a FLAG tag. An adenovirus expressing the green fluorescent protein (GFP) was used as a control. Cells were incubated for 48 h with adenovirus in DMEM supplemented with 10% foetal bovine serum, and the medium was replaced with 0.5% FBS supplemented DMEM. Human aortic VSMCs were obtained from Lonza Sales Ltd. (Basel, Switzerland), cultured in Smooth Muscle Growth Medium-2 (SmGM-2) containing 5% foetal bovine serum, and used between passages 3 and 6. For  $\alpha_v$  knockdown, human VSMCs were transfected with siRNA directed against  $\alpha_v$  or the negative control using a magnet-assisted transfection reagent as previously described.<sup>20</sup> For CD109 overexpression, cells were

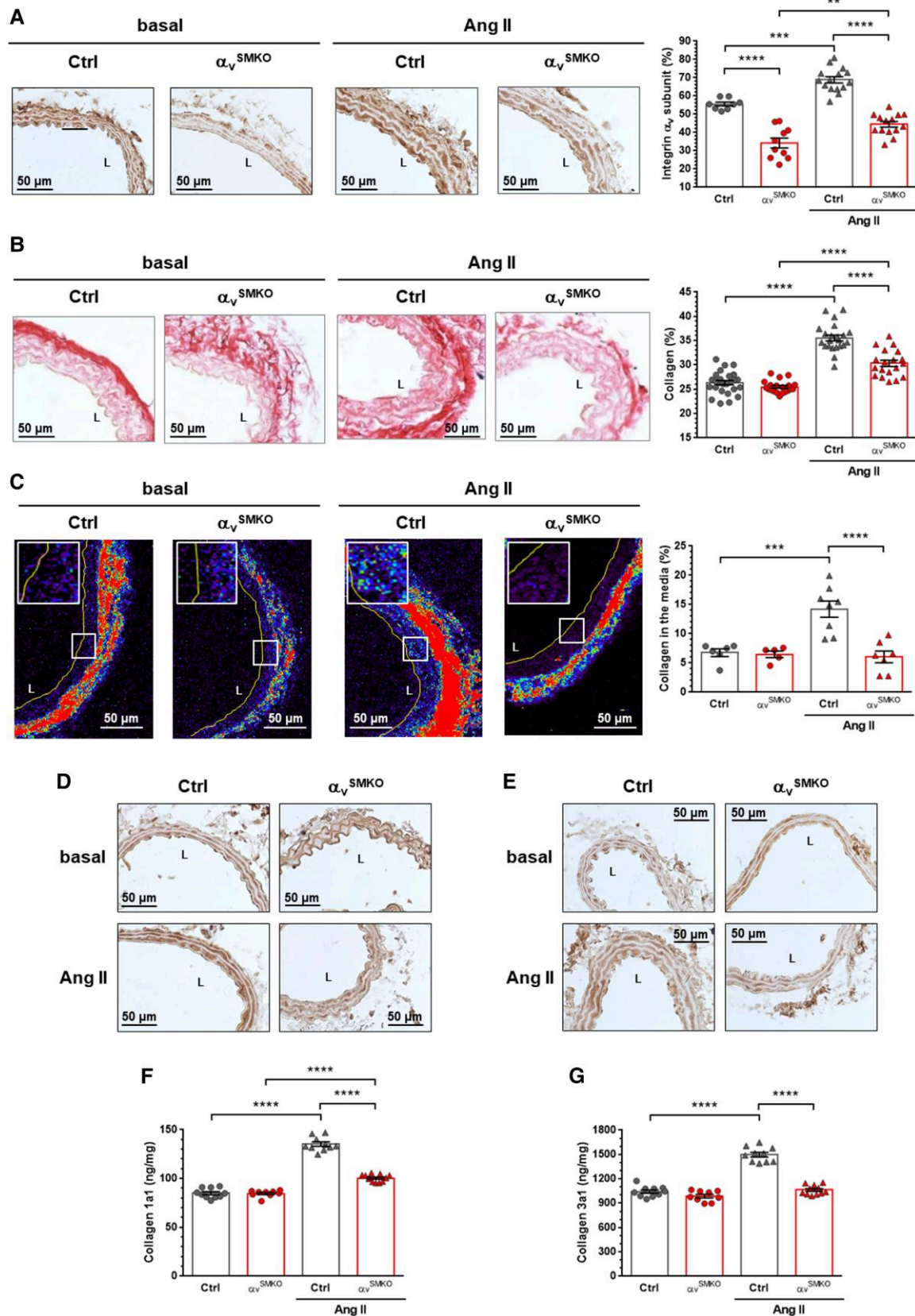


**Figure 1** Knockout of  $\alpha_v$  integrin subunit reduced collagen accumulation in response to 4-week Ang II infusion in  $\alpha_v$  SMKO mice. (A) Immunohistochemistry of the  $\alpha_v$  integrin subunit. Data are presented as mean  $\pm$  SEM ( $n = 8-15$  per group). (B) Cross sections of the carotid artery (continued)

transfected with the adenovirus expressing mouse CD109 and containing a FLAG tag as described above. Vascular smooth muscle cells were then treated with saline, 200 nM Ang II or 2 ng/mL TGF- $\beta$ 1 for 30 min or 48 h.

## Western blot and enzyme-linked immunosorbent assay (ELISA)

Total protein was extracted from frozen carotids or cultured VSMCs. Carotids were homogenized using a Kinexus lysis buffer (mmol/L: MOPS, 20 pH 7.2; EGTA, 2; EDTA, 5; NaF, 30;  $\beta$ -glycerophosphate, 40; sodium pyrophosphate, 20; NaVO<sub>4</sub>, 1; PMSF, 1; containing 0.5% Nonidet P-40; and protease inhibitors cocktail (Sigma)). Vascular smooth muscle cells were scraped with the same buffer. Extracts were centrifuged at 14 000 rpm for 10 min at 4°C, and protein concentration in the supernatant was determined by the Bradford protein assay (Bio-Rad). Proteins (20  $\mu$ g) were separated by 4–15% gradient polyacrylamide gel and transferred to nitrocellulose membranes. Detection of proteins with specific antibodies (see [Supplementary material online, Table S8](#)) was performed as described previously.<sup>18</sup> ELISA assays were performed using different commercial kits (see [Supplementary material online, Table S7](#)) according to manufacturer instructions.

## Microarray analysis

Total RNA was isolated from the aorta of three control and three  $\alpha_v^{\text{SMKO}}$  mice with the RNeasy fibrous tissue kit (Qiagen). Microarray analysis for each genotype and treatment was performed with three samples, each hybridized to one Affymetrix GeneChip® Mouse Exon 1.0 ST Array (Affymetrix, Santa Clara, CA) by the genomic facility of Cochin Institute (Paris, France) according to Affymetrix guidelines. The differentially regulated transcripts in microarray experiments were analysed using A Gene Annotation & Analysis Resource Metascape (<https://metascape.org>) for Gene Oncology (GO) term and pathways enrichment and the Ingenuity Pathways Analysis (IPA) (current version 51963813, release date 11 March 2020, Ingenuity Systems).

## Quantitative real-time polymerase chain reaction

Total RNA extraction and qRT-PCR were conducted as previously described.<sup>18</sup> The PCR primers are listed in the [Supplementary material online, Table S9](#). Messenger RNA content of target genes was normalized to the expression of D-glyceraldehyde-3-phosphate dehydrogenase (GAPDH).

## Colocalization experiments

Vascular smooth muscle cells were seeded at a density of  $7.5 \times 10^3$  cells/well into eight-well Lab-Tek and allowed to grow for 24 h to reach about 80% confluence. Cells were transfected for  $\alpha_v$  knockdown, CD109 overexpression, or GFP expression as a control. After 48 h,

the medium was replaced with 0.5% FBS supplemented DMEM and saline or 200 nM Ang II for 15 min.

Cells were then fixed for 10 min with 4% paraformaldehyde solution at room temperature and washed three times for 5 min with PBS. Cells were permeabilized and non-specific sites blocked for 1 h at room temperature with PBS—Triton 0.3%—BSA 5%. Cells were incubated overnight at 4°C with antibodies directed against EEA1, CD109, and TGF- $\beta$ -R in PBS—BSA 1%. Following three washes of 5 min each, cells were incubated for 1 h with Alexa 555 anti-goat and Alexa 488 anti-mouse or Alexa 488 anti-rabbit antibodies in PBS—BSA 1% and 4',6-diamidino-2-phénylindole (DAPI). Following three washes of 5 min each, cells were mounted and imaged with a Nikon C2 confocal microscope (objective 60 $\times$ ).

## Statistical analysis

Data are presented as mean  $\pm$  standard error of the mean (SEM) of *n* animals/group or from at least three independent experiments. The Mann–Whitney U-test was used to compare two groups. Two-way ANOVA followed by Tukey's multiple comparisons test was performed when comparing multiple groups. *P*-values <0.05 were considered statistically significant.

## Results

### VSMC-specific inactivation of $\alpha_v$ integrins

We first examined the expression of  $\alpha_v$  and its  $\beta$ -subunit binding partners in carotid arteries both at the RNA and the protein level. We confirmed that *Itgav* gene expression was reduced by 60% in SMC-specific  $\alpha_v$  knockout ( $\alpha_v^{\text{SMKO}}$ ) mice (see [Supplementary material online, Figure S1](#)). There was no modification of *Itga5*, *Itgb1*, and *Itgb3* gene expression, indicating a lack of compensation by other integrins. Expressions of *Acta2* and *Myh11* were not modified in  $\alpha_v^{\text{SMKO}}$  mice. As expected,  $\alpha_v$  integrin subunit and  $\alpha_v\beta_3$  integrin immunofluorescence staining was markedly decreased in  $\alpha_v^{\text{SMKO}}$  mice compared with control (Ctrl) mice (see [Supplementary material online, Figure S1](#)). In contrast, positive immunofluorescence staining was observed for  $\alpha_5$  and  $\beta_1$  integrin subunits in both groups. We then analysed the propensity of Ang II to increase  $\alpha_v$  integrin subunit expression. Ang II significantly increased  $\alpha_v$  integrin subunit in both strains, but its level remained markedly lower in Ang II-treated  $\alpha_v^{\text{SMKO}}$  mice compared with Ang II-treated Ctrl mice ([Figure 1A](#)). Expression of  $\alpha_5$  and  $\beta_1$  integrin subunits reached equally increased levels in both strains after Ang II. Expression of  $\beta_3$  integrin subunit significantly increased in Ctrl mice but not in  $\alpha_v^{\text{SMKO}}$  mice. There was no change for  $\alpha$ -SMA and SM-MHC in response to Ang II in both strains, indicating maintenance of a differentiated state of VSMCs (see [Supplementary material online, Figure S1](#)).

### VSMC $\alpha_v$ integrin depletion protects mice from vascular fibrosis

Ang II raised tail-cuff measured SAP by 27 mmHg (25% increase) in Ctrl mice and 30 mmHg (29% increase) in  $\alpha_v^{\text{SMKO}}$  mice, both increases being statistically significant (see [Supplementary material online, Table S1](#)).

### Figure 1 Continued

stained with Picrosirius Red to allow quantification of collagen content in the media. Representative images (magnification  $\times 40$ ) and quantitative data. Data are presented as mean  $\pm$  SEM (*n* = 19–27 animals per group). L, lumen. (C) Representative SHG images of the collagen fibres and corresponding quantification of the carotid media (magnification  $\times 40$ ). The colour spectrum represents collagen content in media and adventitia. The line delineates the internal media layer. Boxed regions demark the position of the insets for each panel. Data are presented as mean  $\pm$  SEM (*n* = 6–8 per group). (D–E) Immunohistochemistry of Col1a1 and Col3a1, respectively. (F–G) Quantitative expression of Col1a1 and Col3a1 (*n* = 9–11 per group). Two-way ANOVA followed by Tukey's multiple comparisons test was used to analyse multiple group comparisons. \*\**P* < 0.01, \*\*\**P* < 0.001, \*\*\*\**P* < 0.0001.

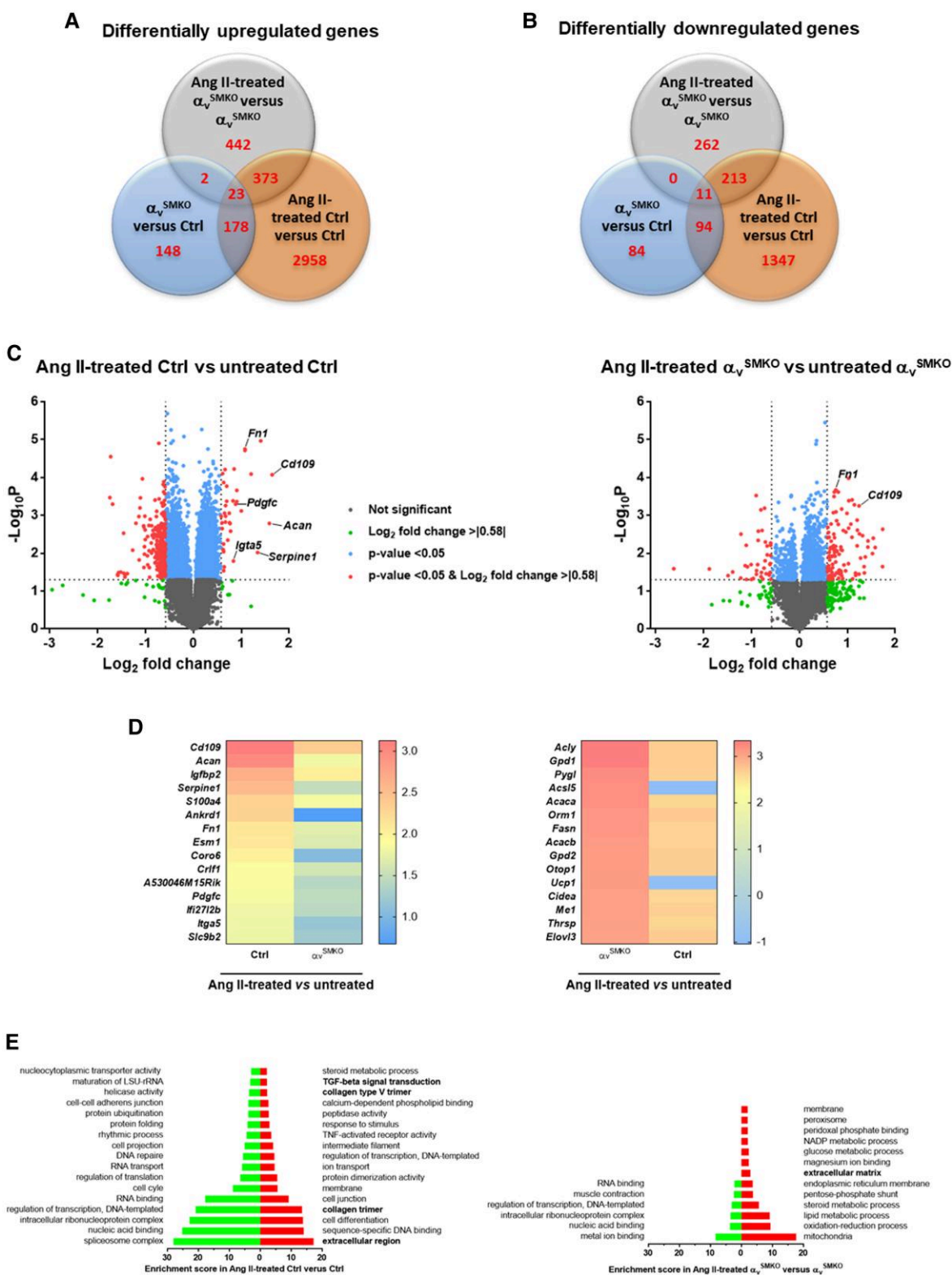


**Figure 2** Transcriptome analysis of thoracic aorta from Ctrl and  $\alpha_v^{\text{SMKO}}$  mice in basal conditions and in response to 4-week Ang II treatment. (A–B) Venn diagram showing the number of genes differentially expressed in  $\alpha_v^{\text{SMKO}}$  vs. Ctrl, Ang II-treated  $\alpha_v^{\text{SMKO}}$  vs.  $\alpha_v^{\text{SMKO}}$ , and Ang II-treated Ctrl vs. Ctrl for upregulated and downregulated genes, respectively. (C) Volcano of plots of comparative of gene expression in Ang II-treated mice. (D) Heatmaps of top 15 differentially upregulated genes. (E) Gene ontology term and pathways enrichment for Ang II-treated Ctrl vs. Ctrl group and Ang II-treated  $\alpha_v^{\text{SMKO}}$  vs.  $\alpha_v^{\text{SMKO}}$ . Left bars indicate downregulated genes and right bars upregulated genes. The terms related to fibrosis (extracellular region, collagen trimer, collagen type V trimer, TGF- $\beta$  signal transduction) are indicated in bold.

Thus, there was no difference between the pressor effects of Ang II in the two strains. Increase in heart rate in response to Ang II was also similar in the two strains. Histological changes in Ang II-treated Ctrl mice included a 1.6-fold increase in MCSA and a 1.2-fold decrease in elastin density. There were no observed differences in these markers between  $\alpha_v^{\text{SMKO}}$  and Ctrl mice.

Sirius Red-stained sections showed increases in collagen in the media of Ctrl mice consistent with the increased arterial pressure (Figure 1B). In particular, collagen density increased 1.35-fold in the Ang II-treated Ctrl group and 1.2-fold in the  $\alpha_v^{\text{SMKO}}$  group. Therefore, the increase in collagen density was 46% less in  $\alpha_v^{\text{SMKO}}$  mice compared with Ctrl mice. SHG imaging based on autofluorescence of collagen further showed that the increase in collagen in the media in Ang II-treated Ctrl mice was absent in Ang II treated- $\alpha_v^{\text{SMKO}}$  mice (Figure 1C). Overall, increasing total collagen in response to Ang II is dramatically less in  $\alpha_v^{\text{SMKO}}$  mice although arterial wall hypertrophy appeared similar to the Ctrl group. Finally, immunohistochemical staining and quantification by ELISA of the predominant collagen subtypes present in the arterial wall, Col1a1 and Col3a1, confirm a marked increase in Ang II-treated Ctrl mice which is strongly reduced in Ang II-treated  $\alpha_v^{\text{SMKO}}$  mice (Figure 1D–G). Besides to collagen expression, the PSR-stained sections revealed further a change in medial collagen repartition in  $\alpha_v^{\text{SMKO}}$  mice in response to Ang II (see Supplementary material online, Figure S2): a decreased percentage of thick (red) fibre area fraction (48% vs. 70%) (see Supplementary material online, Figure S2) and an increased percentage of thin (orange–yellow–green) fibre area fraction (48% vs. 27%) (see Supplementary material online, Figure S2), while no change appeared in Ctrl mice.

## Microarray analysis of profibrotic genes

Given the critical role of TGF- $\beta$  signalling pathways in profibrotic collagen deposition into the arterial wall, a microarray analysis was performed to gain a comprehensive overview of gene expression in the aorta of Ctrl and  $\alpha_v^{\text{SMKO}}$  mice before and after Ang II treatment. Figure 2A and B shows upregulated and downregulated genes, respectively, under basal conditions and in response to Ang II. A total of 351 genes were upregulated, and 189 genes were downregulated in  $\alpha_v^{\text{SMKO}}$  vs. Ctrl. In response to Ang II, 840 genes were upregulated and 486 genes downregulated in  $\alpha_v^{\text{SMKO}}$  mice, while 3532 genes were upregulated and 1665 genes downregulated in Ctrl mice. Angiotensin II infusion differentially upregulated 36 genes in Ang II-treated Ctrl mice and 106 genes in Ang II-treated  $\alpha_v^{\text{SMKO}}$  mice (fold change  $\geq 1.5$  and  $P$ -value  $< 0.05$ ) (Figure 2C). Among these differentially upregulated genes, *Cd109*, *Fn1*, *Acan*, and *Pdgfc* are common to both treatment groups, while other genes encoding proteins potentially involved in fibrosis pathways (*Serpine1* and *Igta5*) were only upregulated and among the top 15 most differentially upregulated genes in the Ang II-treated Ctrl group (Figure 2D and Supplementary material online, Table S2). None of these genes were among the top 15 differentially expressed genes in Ang II-treated  $\alpha_v^{\text{SMKO}}$  mice (Figure 2D and Supplementary material online, Figure S3 and Table S3). When analysing the overlap of the 30 most differentially expressed (upregulated and downregulated) genes between the two comparisons, 13/30 genes differentially expressed in Ang II-treated Ctrl mice were also differentially expressed in Ang II-treated  $\alpha_v^{\text{SMKO}}$  mice (see Supplementary material online, Table S2), while only 2/30 genes differentially expressed in  $\alpha_v^{\text{SMKO}}$  mice were also differentially expressed in Ang II-treated Ctrl mice (see Supplementary material online, Table S3). Functional annotation clustering analysis indicated that Ang II treatment led to higher enrichment scores in Ctrl mice than in  $\alpha_v^{\text{SMKO}}$  mice (Figure 2E) both in upregulated and downregulated genes. Upregulated genes in the Ang II-treated Ctrl group compared with the Ctrl group were enriched in processes related to fibrosis (extracellular region, collagen trimer, TGF- $\beta$  signal transduction) that were not present or had lower scores in the Ang II-treated  $\alpha_v^{\text{SMKO}}$  group compared with the  $\alpha_v^{\text{SMKO}}$  group.

Consistently, Ang II infusion in Ctrl mice increased gene signatures associated with hepatic fibrosis and TGF signalling using IPA (see Supplementary material online, Table S4), while these pathways had much lower scores in Ang II-treated  $\alpha_v^{\text{SMKO}}$  mice. In addition, a total of 70 and 35 genes were differentially expressed in the hepatic fibrosis and TGF signalling pathways, respectively, in Ang II-treated Ctrl mice, whereas only 28 and 7 genes were differentially expressed in Ang II-treated  $\alpha_v^{\text{SMKO}}$  mice (see Supplementary material online, Tables S5 and S6). Altogether, these analyses indicate a lower increase in fibrosis response to Ang II treatment in  $\alpha_v^{\text{SMKO}}$  compared with Ctrl mice.

The microarray analysis revealed *Cd109* coding for a TGF- $\beta$  co-receptor to be one of the most upregulated genes in response to Ang II in both strains (Ctrl  $> 3$ -fold and  $\alpha_v^{\text{SMKO}}$   $> 2$ -fold). This upregulation was validated by conventional quantitative real-time polymerase chain reaction (qRT-PCR) (Table 1). Table 1 also provides detailed values for differentially expressed profibrotic genes encoding collagens and proteins involved in TGF- $\beta$  signalling pathways. As expected, *Igta5* gene expression was significantly higher in Ctrl mice under basal conditions and in response to Ang II compared with  $\alpha_v^{\text{SMKO}}$  mice. At baseline, there was also a lower expression of *Col1a1* gene in  $\alpha_v^{\text{SMKO}}$  mice as compared with Ctrl mice. Following Ang II treatment, in addition to the upregulation of *CD109* gene, *Col1a1* gene expression was increased, and *Tgfb3* gene expression was decreased in both strains. The other studied genes were differentially expressed between the two strains relative to their baseline controls. These included *Igta5*, *Col1a2*, *Col3a1*, *Fn1*, *Tgfb1*, *Tgfb2*, *Tgfb3*, and *Smad3*, which were uniquely increased in Ctrl mice, while *Igfb3*, *Tgfb2*, and *Smad2* were decreased only in  $\alpha_v^{\text{SMKO}}$  mice. Collectively, these findings indicate a downregulation of profibrotic genes in  $\alpha_v^{\text{SMKO}}$  mice as compared with Ctrl mice in response to Ang II and underline the potential importance of *CD109* in Ang II-mediated vascular fibrosis.

## VSMC $\alpha_v$ integrins regulate vascular fibrosis through the TGF- $\beta$ 1–CD109 pathway

To ascertain the crucial role of TGF- $\beta$ 1 signalling and its co-receptor *CD109* in  $\alpha_v$  integrin-mediated vascular fibrosis in response to Ang II, we next assessed expression of TGF- $\beta$ 1, *Smad2/3*, and *CD109* at the protein level. As illustrated in Figure 3A, low immunofluorescence staining of TGF- $\beta$ 1 was found in the media of carotid artery sections at baseline, which was increased in Ctrl mice but not in  $\alpha_v^{\text{SMKO}}$  mice following Ang II treatment. Further supporting differential activation of TGF- $\beta$ 1, ELISA revealed that TGF- $\beta$ 1 was increased only in the aorta of Ctrl mice in response to Ang II (Figure 3B). Western blotting confirmed reduced activation of TGF- $\beta$ 1 signalling in  $\alpha_v^{\text{SMKO}}$  mice as compared with Ctrl mice following Ang II infusion, as indicated by the absence of increased phosphorylation of *Smad2/3* in  $\alpha_v^{\text{SMKO}}$  mice (Figure 3C). As *CD109*, which is known to attenuate TGF- $\beta$ 1 signalling, was found to be upregulated in response to Ang II, we performed immunofluorescence analysis of *CD109* in carotid arteries and ELISA quantitation both in aorta proteins and plasmas. *CD109* expression was clearly elevated in the medial sections of Ang II-treated  $\alpha_v^{\text{SMKO}}$  mice as compared with Ang II-treated Ctrl mice at 28 days (Figure 3D). This result contrasts with the observed upregulation of *Cd109* gene in both strains (Table 1). To more specifically assess early and late upregulation of *CD109* in response to Ang II, *CD109* gene and protein expression were assessed at 4 days after administration of Ang II. The *Cd109* gene was expressed 2.6-fold and 2.3-fold higher at 4 days following Ang II infusion in Ctrl and  $\alpha_v^{\text{SMKO}}$  mice, respectively (data not shown). *CD109* immunofluorescence staining was elevated at 4 days in carotid arteries of both strains (Figure 3D), indicating a stable elevated *CD109* protein expression between 4 and 28 days in  $\alpha_v^{\text{SMKO}}$  mice contrasting with only an early increase in Ctrl mice. Increase in *CD109* protein

**Table 1** Alteration of the gene program in  $\alpha_v^{\text{SMKO}}$  aortas

Gene	Ctrl	$\alpha_v^{\text{SMKO}}$	Ctrl Ang II	$\alpha_v^{\text{SMKO}}$ Ang II
Itgav	1.01 ± 0.09	0.61 ± 0.05**	1.62 ± 0.25*	0.55 ± 0.07**
Itga5	1.02 ± 0.06	1.16 ± 0.13	1.97 ± 0.24**	1.05 ± 0.09
Itgb3	0.97 ± 0.04	0.94 ± 0.09	1.08 ± 0.08	0.63 ± 0.07** #
Col1a1	1.03 ± 0.07	0.71 ± 0.07**	1.92 ± 0.34*	1.28 ± 0.11####
Col1a2	0.97 ± 0.05	1.03 ± 0.07	1.63 ± 0.21**	1.11 ± 0.06
Col3a1	1.00 ± 0.05	1.04 ± 0.07	1.67 ± 0.25**	1.08 ± 0.10
Fn1	1.00 ± 0.06	1.06 ± 0.06	1.88 ± 0.45*	0.86 ± 0.06
Tgfb1	1.03 ± 0.04	0.90 ± 0.09	1.60 ± 0.24*	1.02 ± 0.09
Tgfb2	1.00 ± 0.06	1.13 ± 0.09	1.39 ± 0.11**	1.24 ± 0.09
Tgfb3	0.97 ± 0.05	1.07 ± 0.08	1.23 ± 0.06*	0.90 ± 0.07
Tgfb2	1.00 ± 0.04	1.00 ± 0.04	0.96 ± 0.07	0.76 ± 0.06** #
Tgfb3	1.00 ± 0.05	1.04 ± 0.03	0.72 ± 0.08**	0.65 ± 0.07** ###
Smad2	0.99 ± 0.05	1.02 ± 0.04	1.06 ± 0.06	0.80 ± 0.06* #
Smad3	0.99 ± 0.04	0.89 ± 0.07	1.26 ± 0.10*	0.74 ± 0.06**
Cd109	1.01 ± 0.04	1.16 ± 0.05	3.11 ± 0.49**	2.46 ± 0.46*** ####

Values are expressed as ratio relative to original Ctrl;  $n = 4-5$  in each group. Ang II, angiotensin II; Ctrl, control mice. \* $P < 0.05$ , \*\* $P < 0.01$ , \*\*\* $P < 0.001$  vs. Ctrl; # $P < 0.05$ , ## $P < 0.01$ , ### $P < 0.001$  vs.  $\alpha_v^{\text{SMKO}}$ .

expression in  $\alpha_v^{\text{SMKO}}$  mice at 28 days of Ang II infusion was confirmed in the aortic tissue by ELISA (Figure 3E). Notably, plasma concentration in soluble CD109 was elevated in both strains in response to Ang II (Figure 3F), suggesting that the differential expression between the two Ang II-treated groups in the carotid arteries and aorta was not due to an increased CD109 release in Ctrl mice. Taken together, these data indicate that SMC-specific deletion of  $\alpha_v$  integrins inhibits TGF- $\beta$ 1 signalling in the aorta involving CD109 in response to Ang II.

### Knockdown of $\alpha_v$ integrin or overexpression of CD109 abrogates VSMC phenotypic changes in response to Ang II or TGF- $\beta$ 1 stimulation

Having identified CD109 as a potential regulator of  $\alpha_v$  integrin-mediated vascular fibrosis in response to Ang II, we sought to manipulate expression of  $\alpha_v$  integrin subunit or CD109 to specifically examine effects on *in vitro* VSMC responses to Ang II. To more specifically assess whether production of profibrotic proteins occurred independently of Ang II, we also stimulated VSMCs with TGF- $\beta$ 1. Basal expressions of  $\alpha_v$  integrin subunit were reduced in VSMCs transfected with the Cre-expressing adenovirus-mediating knockdown ( $\alpha_v$ -KD) of  $\alpha_v$  integrin subunit (see Supplementary material online, Figure S4). CD109 protein expression was increased 1.7- and 3.1-fold in Western blot and ELISA, respectively, in VSMCs transfected with an adenovirus expressing mouse CD109 (CD109-OE) compared with VSMCs treated with the empty vector (EV) (see Supplementary material online, Figure S4). Using flow cytometry, we found ~60% of CD109-OE cells expressed the FLAG peptide (see Supplementary material online, Figure S4).

Basal expression of Col1a1 and Col3a1 remained unchanged in  $\alpha_v$ -KD and CD109-OE cells compared with EV cells (Figure 4A and B). Decrease of  $\alpha_v$  integrin subunit expression abrogated the Ang II-induced increase in Col1a1 and Col3a1 expression. Similar to that observed in  $\alpha_v$ -KD cells, the effect of Ang II on these profibrotic proteins was almost completely suppressed in CD109-OE cells. Responses to TGF- $\beta$ 1 stimulation were similar to those of Ang II. Taken together,

these data clearly indicate the predominant role of  $\alpha_v$  integrins and CD109 whether the profibrotic response was initiated with either Ang II or TGF- $\beta$ 1.

To further explore the role of CD109 and  $\alpha_v$  integrin subunit in regulating the TGF- $\beta$  pathway in response to Ang II, we first measured active and latent forms of TGF- $\beta$ . Under basal conditions EV cells expressed similar levels of the active and latent forms (Figure 4C-E). Knockdown of  $\alpha_v$  or overexpression of CD109 has no effect on these ratios. In response to Ang II, knockdown of  $\alpha_v$  or overexpression of CD109 suppressed the increase in active TGF- $\beta$  (Figure 4C). Therefore, overexpression of CD109 gives the same effects as knockdown of  $\alpha_v$ . Angiotensin II-induced upregulation of TGF- $\beta$  resulted in an increase in the latent form (Figure 4D) and therefore a decrease in active/total TGF- $\beta$  (Figure 4E) in  $\alpha_v$ -KD and CD109-OE cells. We next examined the phosphorylation of its intracellular substrates Smad2/3. Angiotensin II and/or TGF- $\beta$ 1-dependent increase in Smad3 phosphorylation observed in EV-treated cells was suppressed in  $\alpha_v$ -KD and CD109-OE cells (Figure 4F).

Further supporting the increased CD109 expression in Ang II-treated  $\alpha_v^{\text{SMKO}}$  mice, membrane-anchored CD109 was increased in  $\alpha_v$ -KD VSMCs in response to Ang II or TGF- $\beta$ 1 (Figure 4G). No additional increase in response to Ang II or TGF- $\beta$ 1 treatment was observed in CD109-OE cells (Figure 4G). This suggests that loss of  $\alpha_v$  causes upregulation of CD109 which makes cells insensitive to the profibrotic effects of Ang II and TGF- $\beta$ .

To further investigate the mechanisms underlying the role of CD109 in vascular fibrosis, we have performed a new set of experiments to evaluate the internalization of TGF- $\beta$  receptor II and CD109 in early endosomes. The fluorescence profile plot of endosomes showed that the signal of the early endosomal marker EEA1 colocalized with the signal of CD109 or TGF- $\beta$ -R in all conditions (Figure 5A and B). This data revealed that CD109 and TGF- $\beta$ -R were internalized in early endosomes. The number of cells with endosomes and the number of endosomes colocalizing EEA1 with CD109 or TGF- $\beta$ -R were quantified, but no significant differences were detected. The knockdown of  $\alpha_v$  compared to the control EV induced a significant decrease of the surface of EEA1/CD109 colocalizing endosomes in response to Ang II and TGF- $\beta$  stimulation (Figure 5C). With the overexpression of CD109, the surface of



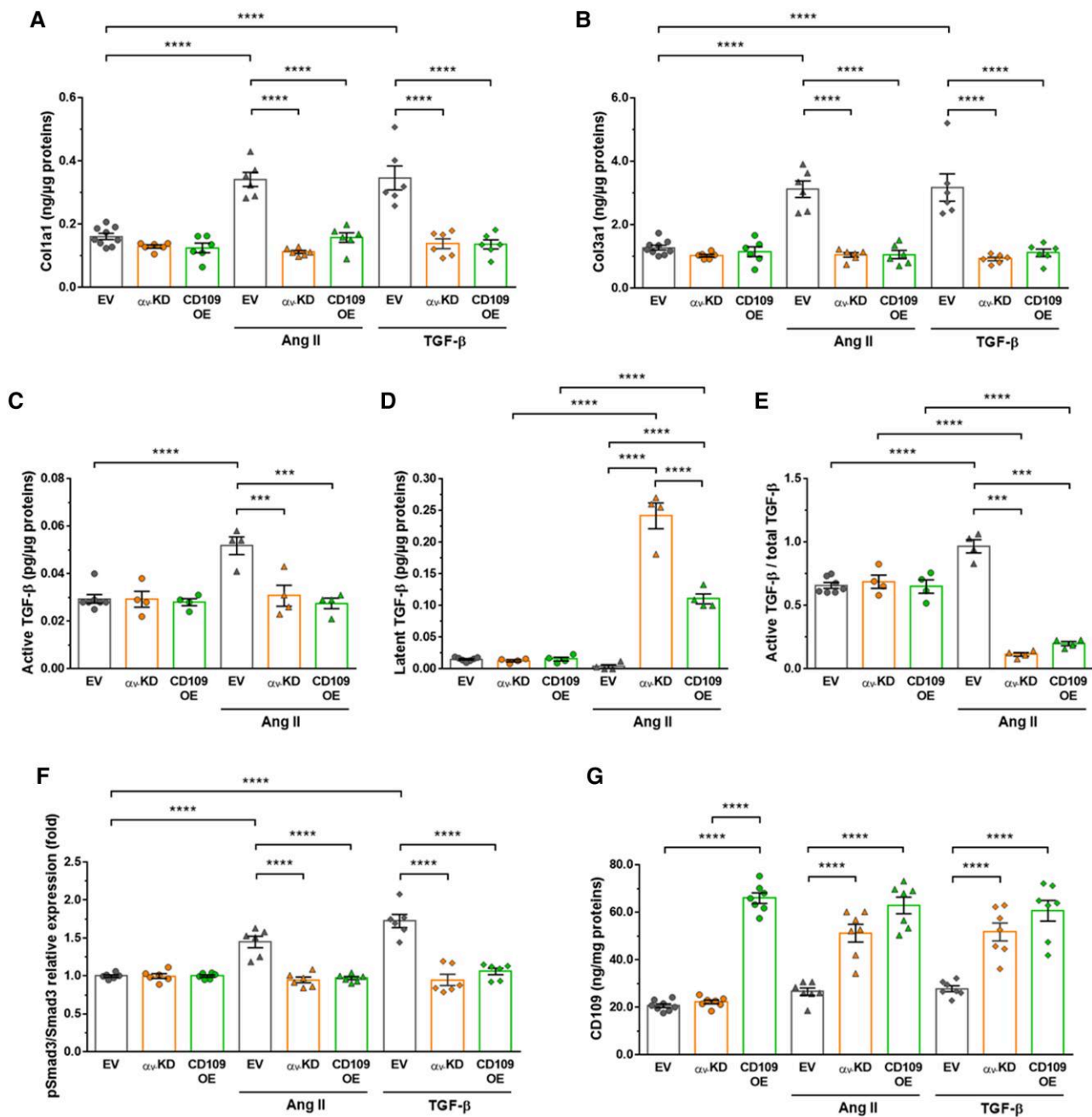


**Figure 4** Knockdown of  $\alpha_v$  integrin subunit or overexpression of CD109 inhibited murine primary VSMC responses to Ang II or TGF- $\beta$ 1. (A–B) Quantification of Col1a1 and Col3a1 by ELISA in lysates of VSMCs transfected with the empty vector (EV), a vector containing Cre-expressing adenovirus ( $\alpha_v$ -KD) or an adenovirus expressing mouse CD109 (CD109-OE) treated for 48 h with Ang II or TGF- $\beta$ 1. (C–E) Quantification active and latent TGF- $\beta$  by ELISA in lysates of EV or  $\alpha_v$ -KD VSMCs treated for 48 h with Ang II. (F–G) Quantification of phosphorylated Smad3 and CD109 in EV,  $\alpha_v$ -KD, or CD109-OE VSMCs treated for 48 h with Ang II or TGF- $\beta$ 1. All data are presented as mean  $\pm$  SEM ( $n = 4–10$  per group). Two-way ANOVA followed by Tukey's multiple comparisons test was used to analyse multiple group comparisons. \*\*\* $P < 0.001$ , \*\*\*\* $P < 0.0001$ .

EEA1/CD109 colocalizing endosomes increased significantly in response to either Ang II or TGF- $\beta$  stimulation. Similarly, with the TGF- $\beta$  stimulation, the surface of EEA1/TGF- $\beta$ -R colocalizing endosomes decreased with the knockdown of  $\alpha_v$  and increased with the overexpression of CD109 (Figure 5D). With the Ang II stimulation, the surface of EEA1/TGF- $\beta$ -R colocalizing endosomes remained similar

in all conditions. These results confirm that  $\alpha_v$  and CD109 are important in Ang II and TGF- $\beta$  signalling by inducing TGF- $\beta$ -R and CD109 internalization in endosomes.

Cellular experiments have been repeated with human VSMCs. As human cells are not floxed for  $\alpha_v$ , we used a siRNA approach to invalidate this integrin (see Supplementary material online, Figure S4). As we have demonstrated

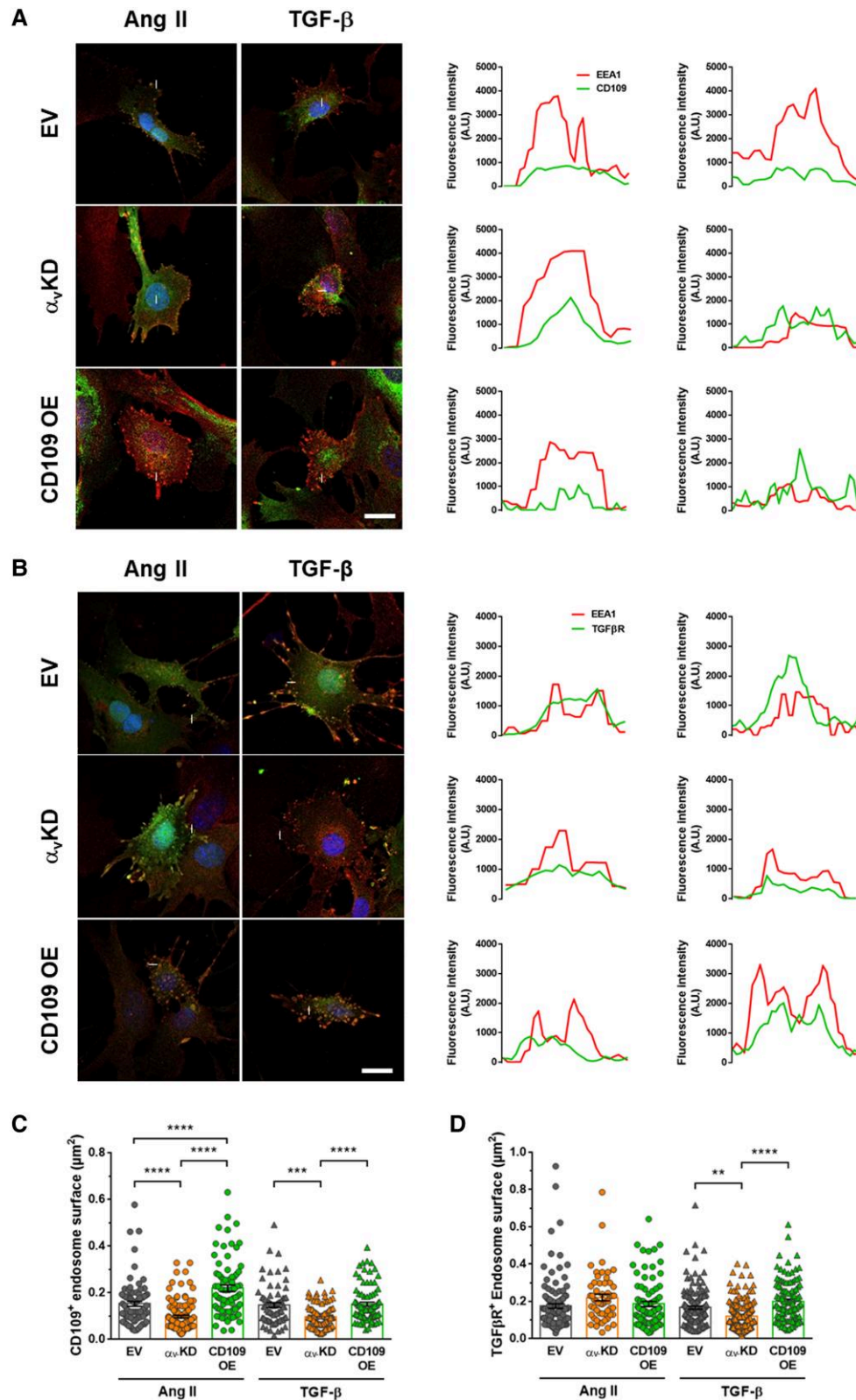


**Figure 5** CD109 and TGF- $\beta$  receptor colocalization with endosomal EEA1. (A) EEA1 and CD109 immunofluorescent staining. Colocalization of EEA1 and CD109 was assessed by confocal microscopy. The fluorescence profile plot along the line indicated on each image was analysed for each protein (graphics on the right). (B) EEA1 and TGF- $\beta$ -R immunofluorescent staining. Colocalization of EEA1 and CD109 was assessed by confocal microscopy. (C) EEA1/CD109 endosome surface measured after 15 min of stimulation with Ang II or TGF- $\beta$ . Scale bar: 5  $\mu\text{m}$ . Two-way ANOVA followed by Tukey's multiple comparisons test was used to analyse multiple group comparisons. \*\* $P < 0.01$ , \*\*\* $P < 0.001$ , \*\*\*\* $P < 0.0001$ .

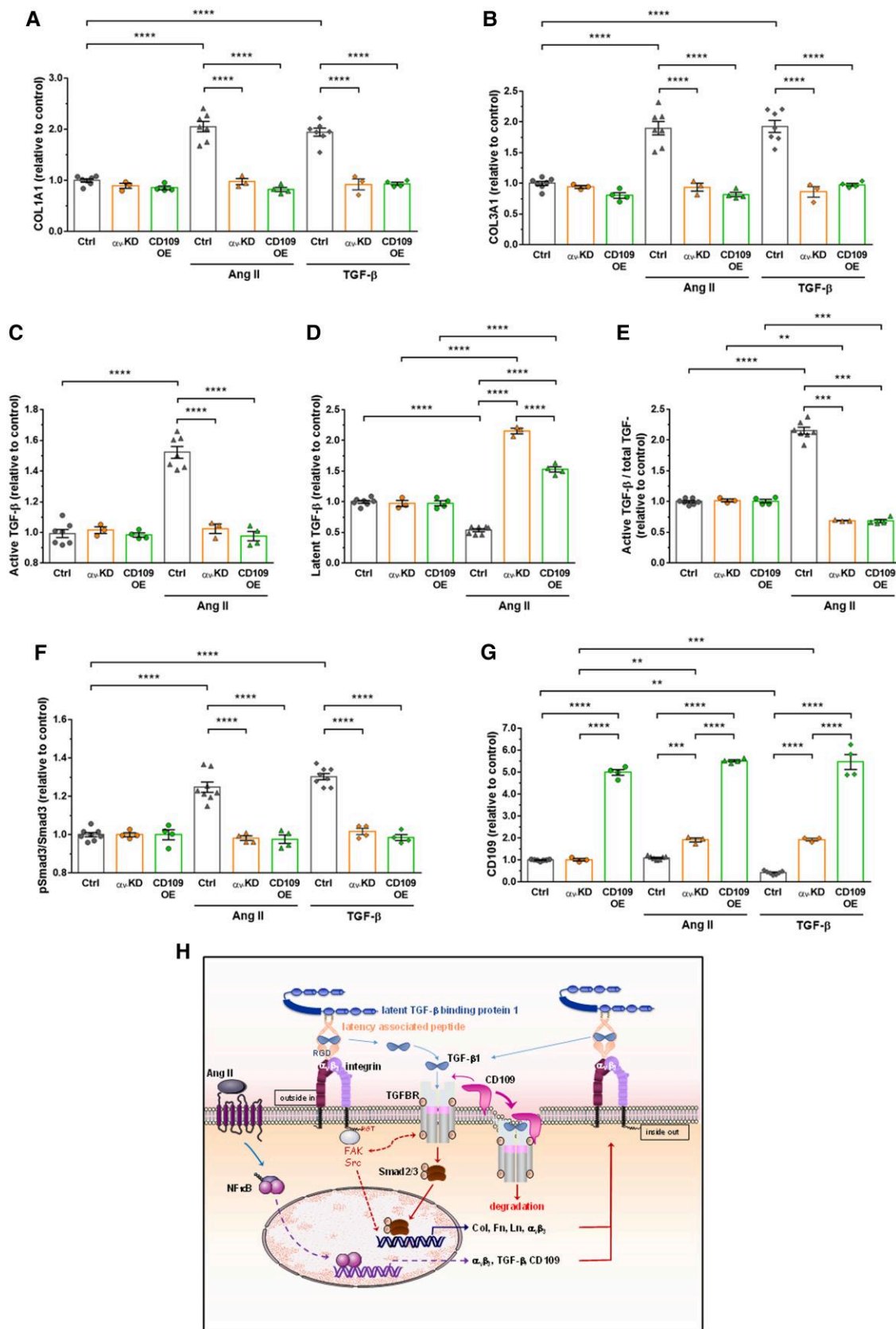


**Figure 6** Knockdown of  $\alpha_v$  integrin subunit or overexpression of CD109 inhibited human aortic VSMC responses to Ang II or TGF- $\beta$ 1. (A–B) Quantification of COL1A1 and COL3A1 by ELISA in lysates of VSMCs transfected with the control siRNA or empty vector (EV), a siRNA against  $\alpha_v$  (continued)

with mouse VSMCs, overexpression of CD109 phenocopied knockdown of  $\alpha_v$  integrin, causing no increase in collagen, active TGF- $\beta$ , Smad3 phosphorylation in response to Ang II or TGF- $\beta$  treatment (Figure 6).

## Discussion

Our findings strongly support the conclusion that deletion of the  $\alpha_v$  integrin subunit from VSMCs protects against Ang II-induced vascular fibrosis. Based on our knowledge of strong expressions of  $\alpha_v$  integrins and TGF- $\beta$  by VSMCs, we considered  $\alpha_v$  integrin-mediated TGF- $\beta$  activation as a key molecular pathway regulating vascular fibrosis in response to Ang II *in vivo*. Our results highlight decreased collagen accumulation in the media of carotid arteries of  $\alpha_v^{\text{SMKO}}$  mice compared with Ctrl mice in response to chronic administration of Ang II. This effect appears independent of haemodynamic changes since arterial pressure is similar in both strains. Using this model, we demonstrated that  $\alpha_v$  integrins are key drivers of vascular fibrosis through TGF- $\beta$  activation/signalling and identified CD109 as a new regulator of TGF- $\beta$  receptor signalling in VSMCs of conduit arteries.

We used the SM22-CreER<sup>T2</sup>(ki) strain to inactivate loxP-flanked  $\alpha_v$  gene with up to 50% efficiency. In this model, tamoxifen-induced recombination has been reported to be specific to smooth muscle cells.<sup>12</sup> Indeed, the level of CreER<sup>T2</sup> mRNA is too low in myofibroblasts to observe efficient recombination.<sup>12</sup> By deleting  $\alpha_v$ , one might expect depletion of all  $\alpha_v$ -containing integrin subunits. However, among the five  $\beta$ -subunit partners of  $\alpha_v$  ( $\beta_1$ ,  $\beta_3$ ,  $\beta_5$ ,  $\beta_6$ , and  $\beta_8$ ), only  $\beta_3$  associated with  $\alpha_v$  in the media *in vivo*.<sup>3</sup> Our data show no changes in  $\beta_3$  subunit expression but as expected a partial reduction in  $\alpha_v\beta_3$  expression, which is remarkably potent for reducing fibrosis in  $\alpha_v^{\text{SMKO}}$  mice. We have not seen any modification of  $\alpha_5$  or  $\beta_1$  subunits of the RGD-recognizing  $\alpha_5\beta_1$  integrin under basal conditions, ruling out any compensation for  $\alpha_v\beta_3$  depletion regarding its canonical role in VSMC adhesion, proliferation, and migration.<sup>3</sup>

Dysregulation of  $\alpha_v$  integrin-mediated TGF- $\beta$  activation and TGF- $\beta$  signalling is arguably major molecular pathways involved in fibrosis in multiple organs. Angiotensin II-mediated vascular fibrosis works via an early ERK1/2-Smad signalling pathway to induce TGF- $\beta$  expression, followed by a late TGF- $\beta$ -dependent Smad3 pathway.<sup>21</sup> In the present study, long-term Ang II administration in  $\alpha_v^{\text{SMKO}}$  mice was used to analyse relationships between TGF- $\beta$  and  $\alpha_v$  expressions in the development of vascular fibrosis. Our findings that loss of  $\alpha_v$  in VSMCs led to a reduction in expression of TGF- $\beta$ -inducible genes and Smad3 phosphorylation in response to Ang II *in vivo* as well as following Ang II or TGF- $\beta$  activation in cell culture support a role for VSMC  $\alpha_v$  integrin-dependent vascular fibrosis. It has been previously reported that such a TGF- $\beta$  activation pathway can be induced by SMC-specific deletion of the LIM (Lin11, Isl-1, and Mec-3) domain protein LIM domain only 7 (LMO7) resulting in increased  $\alpha_v$  and  $\beta_3$  subunit

expression in the vascular wall.<sup>22</sup> We now demonstrate that Ang II triggers *in vivo* vascular fibrosis via  $\alpha_v$  integrins from VSMCs. These data also contrast with a prior study in the kidney showing that dual inhibition of  $\alpha_v\beta_3$  and  $\alpha_v\beta_5$  integrins is required to attenuate renal fibrosis.<sup>5</sup> Our data argue for the involvement of  $\alpha_v\beta_3$  alone in the media of conduit arteries, here shown in the aorta and carotid arteries.

It has been shown that reduction of blood pressure by hydralazine in Ang II infusion reduces fibrosis, hence suggesting that increased accumulation of mural collagen is both mechanical stress mediated and direct Ang II signalling mediated.<sup>23</sup> Mice lacking  $\alpha_1$  had a dramatically reduced fibrosis in Ang II-induced hypertension, largely via reduction of adventitial collagen.<sup>10</sup> In the present study, there is no evidence that haemodynamic factors play a role since arterial pressure and arterial hypertrophy without excessive arterial dilation or dissection are similar in Ctrl and  $\alpha_v^{\text{SMKO}}$  mice. Together, these findings suggest differential actions by different integrins:  $\alpha_1$  integrins acting more via sensing and responding to wall stress and  $\alpha_v$  integrins more via activation of TGF- $\beta$  independently of wall stress.

Extracellular matrix accumulation of collagens I and III is a major contributor to the fibrotic process in response to Ang II infusion. Our histological data indicate that the medial deposition of fibrillar collagen revealed by Red Sirius staining and characterized by scattered amounts using SHG imaging is largely reduced in  $\alpha_v^{\text{SMKO}}$  mice. Increases in medial collagen have been reported to be associated with an increase in larger fibres and a decrease in smaller fibres in aging.<sup>24</sup> Conversely, an intralaminar deposition of thin fibres has been reported in hypertension.<sup>25</sup> Interestingly, using PSR, the collagen fibres in the media tended to be thinner in  $\alpha_v^{\text{SMKO}}$  mice following Ang II infusion, suggesting an incomplete assembly and/or an unbalanced turnover of cross-linked collagen in the absence of VSMC  $\alpha_v$  integrin. RGD-recognizing integrins are well-known collagen-binding receptors responsible for direct binding or indirect binding via bridging molecules to fibrillar collagens to maintain the structural scaffold of the arterial wall.<sup>26</sup> We cannot exclude that SMC-specific deletion of  $\alpha_v$  integrin may have impacted cross-linking of collagen fibrils. However, reduced phosphorylated Smad2/3 signalling associated with reduced collagen synthesis supports a major role for  $\alpha_v$  integrin-mediated activation of latent TGF- $\beta$  in vascular fibrosis. These effects are particularly marked at a late time (28 days), selected to focus on established fibrosis. At such a time,  $\alpha_v\beta_3$  integrin may have a number of roles in addition to simple activation of TGF- $\beta$ , such as promoting matrix deposition/assembly and perhaps synthesis and reactivation of TGF- $\beta$  (Figure 6H). This is also the case for CD109, which goes up early in both strains but stays up only in  $\alpha_v^{\text{SMKO}}$  mice.

Our microarray data revealed differentially expressed genes in  $\alpha_v^{\text{SMKO}}$  mice compared with Ctrl mice, mainly after Ang II infusion. Lack of  $\alpha_v$  integrins decreased the global transcriptional response to Ang II treatment in  $\alpha_v^{\text{SMKO}}$  compared with Ctrl mice. The gene sets and pathways related to fibrosis, such as TGF- $\beta$  signal transduction, collagen type V trimer, collagen trimer, and extracellular region, and the two pathways

### Figure 6 Continued

( $\alpha_v$ -KD) or an adenovirus expressing mouse CD109 (CD109-OE) treated for 48 h with Ang II or TGF- $\beta$ 1. (C–E) Quantification active and latent TGF- $\beta$  by ELISA in lysates of EV or  $\alpha_v$ -KD VSMCs treated for 48 h with Ang II. (F–G) Quantification of phosphorylated Smad3 and CD109 in EV,  $\alpha_v$ -KD, or CD109-OE VSMCs treated for 48 h with Ang II or TGF- $\beta$ 1. All data are presented as mean  $\pm$  SEM ( $n = 3–8$  per group). Two-way ANOVA followed by Tukey's multiple comparisons test was used to analyse multiple group comparisons. \*\*\* $P < 0.001$ , \*\*\*\* $P < 0.0001$ . (H) Schematic model of the mechanism underlying  $\alpha_v$  integrin and TGF- $\beta$ /CD109 signalling cross-talk in Ang II-induced vascular fibrosis. The binding of  $\alpha_v$  integrins to the RGD motif present in LAP leads to the liberation/activation of the TGF- $\beta$  homodimer from its latent complex. After activation, the TGF- $\beta$  homodimer binds to TGF- $\beta$  receptors, thereby initiating TGF- $\beta$ -Smad2/3 signalling, which increases Col, Fn, Ln,  $\alpha_v$  integrins, TGF- $\beta$ , and CD109 expressions. These newly formed integrins will reactivate TGF- $\beta$  from its latent complex, reinforcing the role of TGF- $\beta$  on collagen synthesis. Membrane-anchored CD109 enhances binding of TGF- $\beta$  to TGF- $\beta$  receptors, which in turn promotes internalization of the complex TGF- $\beta$ /TGF- $\beta$  receptor/CD109 and subsequent proteasomal degradation of TGF- $\beta$  receptor. Activation of TGF- $\beta$  in response to Ang II seems independent of circumferential wall stress changes (see text for details).

hepatic fibrosis and TGF signalling are significantly enriched in Ang II-treated compared with Ang II-untreated Ctrl mice. These enrichments were absent or had lower scores in Ang II-treated compared with Ang II-untreated  $\alpha_v^{\text{SMKO}}$  mice. Quantitative PCR analysis confirmed lower upregulation of genes related to integrins, collagen, matrix proteins, and TGF- $\beta$  related and signalling proteins. One of the more pronounced differences in genes affected by Ang II is the upregulation of *CD109* in both strains. We then demonstrated that *CD109* is a new target gene of Ang II in the vascular wall. The role of membrane-anchored CD109 acquires more relevance in fibrogenesis since it antagonizes TGF- $\beta$  signalling.<sup>9,27</sup> Although its role in VSMCs has not been previously studied, CD109 has been linked to TGF- $\beta$  receptor endocytosis and degradation in keratinocytes, skin fibroblasts, cancer cells, and endothelial cells from cerebral microcirculation,<sup>28–32</sup> suggesting that it may potentially act in VSMCs through similar pathways. Notably, we found that CD109 protein is increased in Ctrl mice at 4 days but not at 28 days after Ang II infusion. In  $\alpha_v^{\text{SMKO}}$  mice, CD109 protein remains increased over 28 days. In Ang II-treated Ctrl mice,  $\alpha_v$  integrin-mediated TGF- $\beta$  release likely induces a regulatory mechanism via CD109 leading to internalization and proteasomal degradation of the TGF- $\beta$ /TGF- $\beta$  receptor/CD109 complex. Such a negative regulation does not occur in the absence of activation or reactivation of latent TGF- $\beta$  and subsequent TGF- $\beta$  receptor activation in  $\alpha_v^{\text{SMKO}}$  mice, consistent with the sustained level in CD109 protein and reduced fibrosis at 28 days. It is of interest that CD109 can be released from the cell surface by enzymatic cleavage of the GPI-anchor and that soluble CD109 acts as an antagonist of TGF- $\beta$  signalling.<sup>33</sup> The decrease in CD109 expression in Ctrl mouse media at 28 days compared with 4 days after Ang II administration could therefore also be due partially to CD109 release, in addition to endocytosis and degradation. Our data indicate that soluble CD109 is similarly increased in both strains after 28 days of infusion of Ang II. This finding argues for a degradation of the internalized TGF- $\beta$ /TGF- $\beta$  receptor/CD109 complex rather than a higher release of soluble CD109 in Ang II-treated Ctrl mice. It also supports for the first time a protective role for membrane-anchored CD109 in vascular fibrosis.

Relevant to our *in vivo* findings, knockdown of  $\alpha_v$  integrin or overexpression of CD109 in cultured VSMCs decreased extracellular matrix synthesis and Smad2/3 phosphorylation, supporting the key role of  $\alpha_v$  integrin and CD109 from VSMCs in vascular fibrosis. In an effort to clarify the effect of Ang II-induced integrin-mediated TGF- $\beta$  signalling from a direct effect of TGF- $\beta$  signalling, we exposed cultured VSMCs to Ang II or active TGF- $\beta$ . Our data indicate that both stimuli induce collagen expression as well as TGF- $\beta$  signalling, which are abrogated by  $\alpha_v$  integrin knockdown or CD109 overexpression. Mechanistically, TGF- $\beta$  signalling is likely auto-amplified through integrin transcription, which in turn promotes latent TGF- $\beta$  activation (Figure 6). It is interesting that active TGF- $\beta$  treatment of cultured  $\alpha_v$ -knockdown cells did not induce expression of matrix protein. Transforming growth factor beta addition was used to override the loss of integrin-dependent TGF- $\beta$  activation, so it would have been expected that TGF- $\beta$  treatment would have increased matrix proteins in  $\alpha_v$ -knockdown and control cells similarly. Measures of the latent and active forms of TGF- $\beta$  in Ang II-treated  $\alpha_v$ -knockdown cells support the hypothesis that  $\alpha_v$  knockdown works by blocking TGF- $\beta$  activation. Of note, CD109 overexpression in the presence of  $\alpha_v$  also suppresses TGF- $\beta$  activation in response to Ang II. The increase in the latent form in cells overexpressing CD109 at a lower level than in  $\alpha_v$ -knockdown cells argues for only a partial activation of TGF- $\beta$  by  $\alpha_v$  integrin. This suggests that loss of  $\alpha_v$  integrin causes additional changes in the cell such as upregulation of CD109, which make them insensitive to TGF- $\beta$ . One piece of proof is our data showing an increase in CD109 expression in  $\alpha_v$ -knockdown cells in response to both Ang II and TGF- $\beta$  stimulation. Alternatively, this may be due to loss of a feed-forward loop where TGF- $\beta$  promotes more TGF- $\beta$  production, and activation of this newly synthesized latent TGF- $\beta$  is blocked in  $\alpha_v$ -knockdown cells. Our data suggests that  $\alpha_v$  integrin and

CD109 are important in Ang II and TGF- $\beta$  trafficking by promoting endosome formation and maturation:  $\alpha_v$  knockdown reduces TGF- $\beta$  receptor and CD109 internalization by decreasing endosomes sizes; on the contrary, CD109 overexpression potentializes  $\alpha_v$ -induced TGF- $\beta$  receptor and CD109 internalization with enlarged endosomes.

Clinical perspectives were assessed using human aortic VSMCs with a siRNA approach to knockdown  $\alpha_v$  or an adenovirus approach to overexpress CD109. These translational data clearly showed that the  $\alpha_v$  integrin/TGF- $\beta$ /CD109 axis is functional to regulate vascular fibrosis at the level of VSMCs.

In summary,  $\alpha_v$  integrin-mediated TGF- $\beta$  activation on VSMCs contributes to extracellular matrix deposition in arterial tissues prone to fibrosis in response to Ang II. Involvement of the TGF- $\beta$  signalling pathway and its downregulation by CD109 supports the concept of an important  $\alpha_v$  integrin/TGF- $\beta$ /CD109 axis in Ang II-induced vascular fibrosis. Therapeutic targeting of TGF- $\beta$  is impossible as it is an important factor in many cellular pathways. Therefore, inhibition of TGF- $\beta$  signalling through CD109 may represent a more refined approach to treat vascular fibrosis with fewer unwanted side effects.

## Lead author biography



Patrick Lacolley, MD, PhD, is specialized in cardiology and vascular biology at the Université de Lorraine and Inserm Institute (UMR\_S 1116). His biomedical research is focused on cellular and molecular determinants of arterial stiffness in ageing, hypertension, and thrombophilia with a particular interest on vascular smooth muscle cell biology. The major findings concern cell matrix interactions and mechanosensing linked to haemodynamics in vascular tissue homeostasis.



Zhenlin Li, PhD, is a basic research scientist at the Sorbonne Université, CNRS (UMR 8256), and Inserm Institute (ERL U1164). His research is focused on the function of genes encoding the cytoskeleton proteins and transcription factors in cardiovascular and neuromuscular system as well as their involvement in the development of diseases.

## Authors' contributions

Z.L., A.L.H., V.R., and P.L. designed the study. Z.L., E.B., A.P., H.L., Y.K., J.B., J.G.L., J.D.H., R.B., F.P., V.R., and P.L. performed experiments and analysed results. Z.L., V.R., and P.L. drafted the manuscript. A.L.H., P.C., and J.D.H. revised the manuscript for important intellectual content.

## Data availability

The data underlying this article will be shared on reasonable request to the corresponding author.

## Supplementary material

Supplementary material is available at *European Heart Journal Open* online.

## Acknowledgements

We wish to thank Zhor Ramdane-Cherif, Kenza Benkirane, and Cindy Lerogon for their expert technical assistance. We thank the Imaging Core Facility (PTIBC) of UMS2008/US40 IBSLor (Université de Lorraine-CNRS-INSERM) for their SHG microscopy and the IBPS platform (Sorbonne University) for their confocal microscopy analysis and housing of mice.

## Funding

This work was supported by Future program the Agence Nationale de la Recherche (No ANR-15-RHU-0004 and ANR-13-BSV1-0026); the Contrat Plan État Région, Innovations Technologiques, Modélisation & Médecine Personnalisée, and FEDER (Fonds Européen de Développement Régional); the 'Federation Française de Cardiologie'.

**Conflict of interest:** None declared.

## References

- Henderson NC, Rieder F, Wynne TA. Fibrosis: from mechanisms to medicines. *Nature* 2020;**587**:555–566.
- Harvey A, Montezano AC, Touyz RM. Vascular biology of ageing-implications in hypertension. *J Mol Cell Cardiol* 2015;**83**:112–121.
- Lacolley P, Regnault V, Segers P, Laurent S. Vascular smooth muscle cells and arterial stiffening: relevance in development, aging, and disease. *Physiol Rev* 2017;**97**:1555–1617.
- Robertson IB, Rifkin DB. Regulation of the bioavailability of TGF- $\beta$  and TGF- $\beta$ -related proteins. *Cold Spring Harb Perspect Biol* 2016;**8**:a021907.
- Bagnato G, Irrera N, Pizzino G, Santoro D, Roberts WN, Bagnato G, Pallio G, Vaccaro M, Squadrito F, Saitta A, Altavilla D, Bitto A. Dual  $\alpha v \beta 3$  and  $\alpha v \beta 5$  blockade attenuates fibrotic and vascular alterations in a murine model of systemic sclerosis. *Clin Sci (Lond)* 2018;**132**:231–242.
- Henderson NC, Arnold TD, Katamura Y, Giacomini MM, Rodriguez JD, McCarty JH, Pellicoro A, Raschperger E, Betsholtz C, Ruminski PG, Griggs DW, Prinsen MJ, Maher JJ, Iredale JP, Lacy-Hulbert A, Adams RH, Sheppard D. Targeting of  $\alpha v$  integrin identifies a core molecular pathway that regulates fibrosis in several organs. *Nat Med* 2013;**19**:1617–1624.
- Murray IR, Gonzalez ZN, Baily J, Dobie R, Wallace RJ, Mackinnon AC, Smith JR, Greenhalgh SN, Thompson AI, Conroy KP, Griggs DW, Ruminski PG, Gray GA, Singh M, Campbell MA, Kendall TJ, Dai J, Li Y, Iredale JP, Simpson H, Huard J, Péault B, Henderson NC.  $\alpha v$  integrins on mesenchymal cells regulate skeletal and cardiac muscle fibrosis. *Nat Commun* 2017;**8**:1118.
- Prazeres P, Turquetti AOM, Azevedo PO, Barreto RSN, Miglino MA, Mintz A, Delbono O, Birbrair A. Perivascular cell  $\alpha v$  integrins as a target to treat skeletal muscle fibrosis. *Int J Biochem Cell Biol* 2018;**99**:109–113.
- Bizet AA, Tran-Khanh N, Saksena A, Liu K, Buschmann MD, Philip A. CD109-mediated degradation of TGF- $\beta$  receptors and inhibition of TGF- $\beta$  responses involve regulation of SMAD7 and Smurf2 localization and function. *J Cell Biochem* 2012;**113**:238–246.
- Louis H, Kakou A, Regnault V, Labat C, Bressenot A, Gao-Li J, Gardner H, Thornton SN, Challande P, Li Z, Lacolley P. Role of  $\alpha 1 \beta 1$ -integrin in arterial stiffness and angiotensin-induced arterial wall hypertrophy in mice. *Am J Physiol Heart Circ Physiol* 2007;**293**:H2597–H2604.
- Lu S, Strand KA, Mutryn MF, Tucker RM, Jolly AJ, Furgeson SB, Moulton KS, Nemenoff RA, Weiser-Evans MCM. PTEN (phosphatase and tensin homolog) protects against Ang II (Angiotensin II)-induced pathological vascular fibrosis and remodeling-brief report. *Arterioscler Thromb Vasc Biol* 2020;**40**:394–403.
- Kuhbandner S, Brummer S, Metzger D, Chambon P, Hofmann F, Feil R. Temporally controlled somatic mutagenesis in smooth muscle. *Genesis* 2000;**28**:15–22.
- Lacy-Hulbert A, Smith AM, Tissire H, Barry M, Crowley D, Bronson RT, Roes JT, Savill JS, Hynes RO. Ulcerative colitis and autoimmunity induced by loss of myeloid  $\alpha v$  integrins. *Proc Natl Acad Sci U S A* 2007;**104**:15823–8.
- Galmiche G, Labat C, Mericskay M, Aissa KA, Blanc J, Retailleau K, Bourhim M, Coletti D, Loufrani L, Gao-Li J, Feil R, Challande P, Henrion D, Decaux JF, Regnault V, Lacolley P, Li Z. Inactivation of serum response factor contributes to decrease vascular muscular tone and arterial stiffness in mice. *Circ Res* 2013;**112**:1035–1045.
- López-Andrés N, Calvier L, Labat C, Fay R, Diez J, Benetos A, Zannad F, Lacolley P, Rossignol P. Absence of cardiostrophin 1 is associated with decreased age-dependent arterial stiffness and increased longevity in mice. *Hypertension* 2013;**61**:120–129.
- Bersi MR, Collins MJ, Wilson E, Humphrey JD. Disparate changes in the mechanical properties of murine carotid arteries and aorta in response to chronic infusion of angiotensin-II. *Int J Adv Eng Sci Appl Math* 2013;**4**:228–240.
- Eberth JF, Gresham VC, Reddy AK, Popovic N, Wilson E, Humphrey JD. Importance of pulsatility in hypertensive carotid artery growth and remodeling. *J Hypertens* 2009;**27**:2010–2021.
- Langlois B, Belozertseva E, Parlakian A, Bourhim M, Gao-Li J, Blanc J, Tian L, Coletti D, Labat C, Ramdane-Cherif Z, Challande P, Regnault V, Lacolley P, Li Z. Vimentin knock-out results in increased expression of sub-endothelial basement membrane components and carotid stiffness in mice. *Sci Rep* 2017;**7**:11628.
- Gluais M, Clouet J, Fusellier M, Decante C, Moraru C, Dutilleul M, Veziers J, Lesoeur J, Dumas D, Abadie J, Hamel A, Bord E, Chew SY, Guicheux J, Le Visage C. *In vitro* and *in vivo* evaluation of an electrospun-aligned microfibrillar implant for Annulus fibrosus repair. *Biomaterials* 2019;**205**:81–93.
- Lagrange J, Worou ME, Michel JB, Raoul A, Didelot M, Muczynski V, Legendre P, Plénat F, Gauchotte G, Lourenco-Rodrigues MD, Christophe OD, Lenting PJ, Lacolley P, Denis CV, Regnault V. The VWF/LRP4/ $\alpha v \beta 3$ -axis represents a novel pathway regulating proliferation of human vascular smooth muscle cells. *Cardiovasc Res* 2022;**118**:622–637.
- Wang W, Huang XR, Canlas E, Oka K, Truong LD, Deng C, Bhowmick NA, Ju W, Bottlinger EP, Lan HY. Essential role of Smad3 in angiotensin II-induced vascular fibrosis. *Circ Res* 2006;**98**:1032–1039.
- Xie Y, Ostriker AC, Jin Y, Hu H, Sizer AJ, Peng G, Morris AH, Ryu C, Herzog EL, Kyriakides T, Zhao H, Dardik A, Yu J, Hwa J, Martin KA. LMO7 is a negative feedback regulator of transforming growth factor  $\beta$  signaling and fibrosis. *Circulation* 2019;**139**:679–693.
- Wu J, Thabet SR, Kirabo A, Trott DW, Saleh MA, Xiao L, Madhur MS, Chen W, Harrison DG. Inflammation and mechanical stretch promote aortic stiffening in hypertension through activation of p38 mitogen-activated protein kinase. *Circ Res* 2014;**114**:616–625.
- Ferruzzi J, Madziva D, Caulk AW, Tellides G, Humphrey JD. Compromised mechanical homeostasis in arterial aging and associated cardiovascular consequences. *Biomech Model Mechanobiol* 2018;**17**:1281–1295.
- Bersi MR, Bellini C, Wu J, Montaniel KRC, Harrison DG, Humphrey JD. Excessive adventitial remodeling leads to early aortic maladaptation in angiotensin-induced hypertension. *Hypertension* 2016;**67**:890–896.
- Zeltz C, Orgel J, Gullberg D. Molecular composition and function of integrin-based collagen glues-introducing COLINBRIs. *Biochim Biophys Acta* 2014;**1840**:2533–2548.
- Yokoyama M, Ichinoe M, Okina S, Sakurai Y, Nakada N, Yanagisawa N, Jiang SX, Numata Y, Umezawa A, Miyazaki K, Higashihara M, Murakumo Y. CD109, a negative regulator of TGF- $\beta$  signaling, is a putative risk marker in diffuse large B-cell lymphoma. *Int J Hematol* 2017;**105**:614–622.
- Fessel J. Caveolae, CD109, and endothelial cells as targets for treating Alzheimer's disease. *Alzheimers Dement (N Y)* 2020;**6**:e12066.
- Finnson KW, Tam BY, Liu K, Marcoux A, Lepage P, Roy S, Bizet AA, Philip A. Identification of CD109 as part of the TGF-beta receptor system in human keratinocytes. *FASEB J* 2006;**20**:1525–1527.
- Man XY, Finnson KW, Baron M, Philip A. CD109, a TGF- $\beta$  co-receptor, attenuates extracellular matrix production in scleroderma skin fibroblasts. *Arthritis Res Ther* 2012;**14**:R144.
- Vorstenbosch J, Al-Ajmi H, Winocour S, Trzeciak A, Lessard L, Philip A. CD109 over-expression ameliorates skin fibrosis in a mouse model of bleomycin-induced scleroderma. *Arthritis Rheum* 2013;**65**:1378–1383.
- Zhang JM, Murakumo Y, Hagiwara S, Jiang P, Mii S, Kalyoncu E, Saito S, Sakurai Y, Numata Y, Yamamoto T, Takahashi M. CD109 attenuates TGF- $\beta 1$  signaling and enhances EGF signaling in SK-MG-1 human glioblastoma cells. *Biochem Biophys Res Commun* 2015;**459**:252–258.
- Li C, Hancock MA, Sehgal P, Zhou S, Reinhardt DP, Philip A. Soluble CD109 binds TGF- $\beta$  and antagonizes TGF- $\beta$  signalling and responses. *Biochem J* 2016;**473**:537–547.